WILEY InterScience® DISCOVER SOMETHING GREAT

PROTEINS STRUCTURE ■ FUNCTION ■ BIOINFORMATICS

NMR study and molecular dynamics simulations of optimized β-hairpin fragments of protein G

Yun Wei,[1] Beatrice M. P. Huyghues-Despointes,[2] Jerry Tsai,[1] and J. Martin Scholtz[1,2]*

[1] Department of Biochemistry and Biophysics, Texas A&M University, College Station, Texas

[2] Department of Molecular and Cellular Medicine, Texas A&M Health Science Center, College Station, Texas

ABSTRACT

The stability and structure of several β-hairpin peptide variants derived from the C-terminus of the B1 domain of protein G were investigated by a number of experimental and computational techniques. Our analysis shows that the structure and stability of this hairpin can be greatly affected by one or a few simple mutations. For example, removing an unfavorable charge near the N-terminus of the peptide (Glu42 to Gln or Thr) or optimization of the N-terminal charge–charge interactions (Gly41 to Lys) both stabilize the peptide, even in water. Furthermore, a simple replacement of a charged residue in the turn (Asp47 to Ala) changes the β-turn conformation. Finally, we show that the effects of combining these single mutations are additive, suggesting that independent stabilizing interactions can be isolated and evaluated in a simple model system. Our results indicate that the structure and stability of this β-hairpin peptide can be modulated in numerous ways and thus contributes toward a more complete understanding of this important model β-hairpin as well as to the folding and stability of larger peptides and proteins.

Proteins 2007; 69:285–296.

***Key words:* β-hairpin; NMR; β-turn; β-hairpin conformation; electrostatic interactions; peptide design; simulations; hairpin register.**

INTRODUCTION

Some short peptide fragments excised from proteins can fold autonomously in aqueous solution into native-like conformations in the absence of interactions with other structural elements.[1,2] These polypeptide fragments may thus play important roles in initiating protein folding by narrowing the conformational search path to one where local effects dominate the interactions during the early stages of protein folding.[3–5] To further understand early events in protein folding, short peptides have often been used as simple model systems to identify specific noncovalent interactions that are crucial to secondary structure formation.[6–11] Many features of protein folding have also been observed in the folding of peptide models, including the general hydrophobic collapse, close packing of side chains, and the formation of intramolecular hydrogen bonds.[6–8,12,13] For example, over the last couple of decades, model peptides have been used quite successfully to identify local interactions and determine their contributions to the formation and stability of the α-helix.[14–16] Similar studies on the formation of simple β-hairpins, the minimal unit of the β-sheet structure, have lagged behind and have been hampered by the marginal stability of the structure and the strong tendency of the peptides to aggregate.

Fortunately, the last decade has seen considerable progress in our understanding of β-sheet and β-hairpin formation with the developments of well-folded "designed β-hairpin" systems, often employing amino acid mimics as key building blocks; a recent review summarizes some of the important findings.[17] There are several key interactions and features of the peptides that appear to be critical to the folding and stability of β-sheets and β-hairpins. Briefly, the specific nature and propensity of residues in the β-turn itself has been shown to be important in defining the conformation and stability of model β-hairpin peptides. Griffiths-Jones *et al.*[18] have shown that significant β-turn conformation is still populated in a truncated variant of their model β-hairpin peptide in the absence of interstrand hydrophobic contacts, suggesting the intrinsic turn propensity plays an important role in nucleating β-hairpin folding. In a separate study with a different model peptide, de Alba *et al.*[19,20] demonstrated that a peptide can fold in aqueous solution to two β-hairpin structures that can coexist in equilibrium and single-residue substitutions in the β-turn region can dramatically alter the preferences between the β-turn conformations.[19–21] These results demonstrate the important role of the β-turn sequence in

The Supplementary Material referred to in this article can be found online at http://www.interscience.wiley.com/jpages/0887-3585/suppmat/

Grant sponsor: Robert A. Welch Foundation; Grant numbers: BE-1281, A-1549.

*Correspondence to: J. Martin Scholtz, 440 Reynolds Medical Building, Texas A&M Health Science Center, College Station, TX 77843–1114. E-mail: jm-scholtz@tamu.edu

Received 5 September 2006; Revised 20 February 2007; Accepted 27 February 2007

Published online 28 June 2007 in Wiley InterScience (www.interscience.wiley.com). DOI: 10.1002/prot.21494

determining both the stability and conformational preferences of the β-hairpin.[9,22]

In addition to studies on designed, de novo β-sheet and β-hairpin peptides, there have been a few studies on peptides derived directly from proteins and thus comprised of native residues with interactions that are probably more biologically relevant. To our knowledge, the first reported β-hairpin peptide that was demonstrated to autonomously fold into a native-like structure was the 17-residue peptide from the N-terminus of ubiquitin, however, this peptide only adopts ~20% β-hairpin conformation in aqueous solution.[2,23] A major breakthrough in the study of β-hairpin formation came when Serrano and coworkers showed that the 16-residue peptide corresponding to the C-terminal hairpin (residues 41–56, known here as G-hairpin, proposed first by Kobayashi *et al.*[24]) of B1 domain of the streptococcal protein G (PGB1) populates up to ~40% of a monomeric, native-like β-hairpin structure in aqueous solution.[1,9]

Since this original discovery, the G-hairpin has been the paradigm for β-hairpin formation using experimental (NMR, CD spectroscopy)[1,10,25–29] and computational[30–35] approaches. These studies have led to the suggestions that there are four main factors that contribute to the folding and stability of the G-hairpin: (1) the intrinsic β-turn propensities of the turn residues,[9,36] (2) hydrophobic interactions between the side chains across the β-strands,[12,26,37] (3) interstrand hydrogen bonds that help define and maintain the architecture of the hairpin,[31] and (4) polar side-chain to side-chain (sc-sc) interactions, including electrostatic interactions and salt bridges.[10,11,20,29] Among these, the interstrand hydrophobic interactions between the aromatic groups of Trp43, Tyr45, Phe52, and the nonpolar residue Val54 have been suggested to provide the largest contribution to stability and have even been implicated as the nucleation site for folding.[32,34,35,38]

Most previous studies using the G-hairpin as the reference model for β-hairpin structure have focused on either the interstrand hydrophobic interactions or on optimization of the whole loop sequence to increase the stability. The hydrophobic cluster of G-hairpin is formed between a valine (Val54) side chain and the rings of three aromatic residues (Trp43, Tyr45, and Phe52). In one elegant study to explore hydrophobic interactions, Cochran *et al.* have shown replacements of the other three residues in the hydrophobic cluster with tryptophan significantly stabilize the G-hairpin, thus demonstrating that these interactions could be transferred from another model system that they called the tryptophan zipper.[26] Kobayashi *et al.* showed single mutations to alanine of either Trp43, Tyr45, or Phe52 in the hydrophobic core can dramatically destabilize the G-hairpin.[10]

In intact PGB1, the second β-turn region consists of a six-residue loop (DDATKT) that forms a 4:4 hairpin with a type IV turn in the protein structure according to the nomenclature of Thornton.[39,40] The loop is closed by two hydrogen bonds formed between Asp46 and Thr51 in the protein, whereas only one hydrogen bond between Asp46 NH and Thr51 carboxyl is possible in the peptide. The β-turn of G-hairpin is a long loop and presumably more flexible and entropically unfavorable compared to short and rigid β-turns.[27,36] Fesinmeyer *et al.* has shown that replacing the native turn with NPATGK, a sequence selected by comparisons to known turns, can substantially enhance the stability of the resulting G-hairpin variant.[27] In fact, replacement of the six-residue loop with the shorter turn-favoring sequence Val-$_D$Pro-Gly-Lys in the context of hydrophobic cluster from the G-hairpin is stabilizing.[36,41] McCallister *et al.* have examined the effects of replacing the turn residues Asp46, Asp47, Thr49, or Thr51 with alanine in the protein G and the D47A mutation is the only one found stabilizing the protein.[42] Also, the replacement of Asp47 at turn position *i* with Ala is the only single loop mutation reported that stabilizes the G-hairpin.[10,42] The fact that the D47A mutation stabilizes the G-hairpin peptide is quite unexpected, because the D47A mutation removes not only a salt bridge with Lys50 across the turn, but also a hydrogen bond between Asp47 and Tyr45. However, no explanation for the increased in the stability of peptide has been given.

Single amino acid substitutions that reverse or remove the charges on solvent-exposed side chains have been shown to sometimes give increases in protein stability without altering the structure.[43,44] Similarly, the pH and salt-dependence of β-hairpin formation in a number of model systems suggest that long- and short-range electrostatic interactions across β-strands can also contribute to stability.[29,45–47] It has also been shown both in designed peptides and G-hairpin that enhanced electrostatic interactions at the terminal positions of the peptide can contribute to the stability of the β-hairpin.[29,48] Additionally, the introduction of cross-strand Lys-Glu ion pairs near the terminal regions of designed β-hairpins also show increased stability.[46,48] However, these mutations might also create additional hydrophobic interactions due to the long hydrophobic side chain of Lys and it is difficult to separate these contributions to stability from the ion-pair interactions.

Our goal in this study is to combine known mutations with a few new ones to make a more stable G-hairpin and determine the energetic contributions of the different types of interactions. To gain further insights into how long-range coulombic interactions and hydrophobic interactions stabilize the β-hairpin, we investigated several replacements (E42T/E42Q/D47A) that remove the unfavorable interactions without introducing new hydrophobic interactions in the G-hairpin model system. Since the turn has such an important role in β-hairpin folding, we also provide structural studies of the peptides using 2D NMR spectroscopy. Surprisingly, we find that single mutations can have rather large effects on not only stability (not so

 DOI 10.1002/prot

unexpected), but also on structure. This observation appears to be more pronounced in β-strands than in α-helical peptide models or in proteins, where single amino acid changes almost never result in large or even detectable structural changes. Molecular dynamics modeling for each peptide variant was also performed to give us insights into structural features and to support and augment the NMR studies.

MATERIALS AND METHODS

Peptides synthesis and purification

The peptides were synthesized using Fmoc chemistry with HBTU activation and standard solid-phase methods on Wang Resin. Peptides were cleaved from the resin and deprotected by a mixture of 90% TFA, 5% thioanisole, 3% ethanedithiol, and 2% anisole. The peptides were purified using reversed-phase FPLC on a Pharmacia Source 15RPC column with two gradient runs of acetonitrile and 5 m*M* sodium phosphate or 10 m*M* ammonium bicarbonate.[29] The peptide identities were confirmed by MALDI mass spectrometry.

NMR spectroscopy

The NMR samples (∼1 m*M*) were prepared as described previously[29] in a volume of 0.75 mL either in a mixture of H_2O/D_2O (9:1 ratio by volume) or 99.8% D_2O buffered with 5 m*M* sodium phosphate. The pH was adjusted to 7 with a small addition of DCl or NaOD and measured by a PHM-220 pH meter with a combined glass electrode. The pH was not corrected for solvent isotope effects. All NMR experiments were acquired with 500 MHz Varian Inova spectrometers and processed with NMRPipe.[49] The temperature of the NMR probe was calibrated using the temperature dependent chemical shifts (difference between the methyl and hydroxyl resonances) of a 100% (v/v) methanol standard.[50] Sodium 2,2-dimethyl-2-silapentane-5-sulfonate was used as an internal reference and set to 0 ppm for all temperatures and cosolvent concentrations. The thermal dependences of ^1H chemical shifts of the peptides in D_2O at pH 7 were determine from 1D NMR spectra obtained by accumulating 128 scans with 4096 complex points and spectral width of 6000. Measurements were taken with increasing temperature from 2 to 27°C at ∼2°C intervals and from 30 to 80°C at ∼5°C intervals. The thermal dependence of ^1H chemical shifts of the K41+T42+A47 peptide in D_2O in 20% methanol was obtained at a wider temperature range (−2 to 80°C). A combination of TOCSY and NOESY 2D-NMR spectra was used to assign all resonances. A mixing time of 200 ms was used for NOESY spectra in both D_2O and 9:1 mixture of H_2O/D_2O solutions. The TOCSY experiments used a mixing time of 80 ms.

Thermal melting curves by 1D NMR

The chemical shifts of Tyr45 Cδ protons were chosen in this study as the probe to determine the relative stabilities of G-hairpin variants. We chose Tyr45 Cδ proton because a large signal change was observed with temperature, in agreement with what has been observed previously.[25,29] The changes in chemical shift with temperature were analyzed assuming a two-state folding transition between folded and unfolded β-hairpins, as previously described.[29] The cosolvent methanol, known to stabilize secondary structure in peptides,[11] was used to help define the folded state pre-transition baseline (5.98 ppm) by following thermal transition in 20% methanol for the most stable peptide (K41+T42+A47) from temperatures below 0°C (∼ −2°C). The unfolded baseline value (6.86 ppm) of Tyr45 Cδ proton was determined by fitting the chemical shift values of Tyr45 Cδ proton of an unfolded G-hairpin variant at high temperatures in a previous study.[25,29]

Molecular dynamics simulation

Using the ENCAD program and potential energies with the F3C water model,[51,52] MD simulations were performed on all peptide variants, as described previously.[29] The coordinates of the starting structure used those for the β-hairpin in the crystal structure of PGB1 (pdb: 1PGB). The peptide was placed in a periodic box of water without boundaries[51,52] and the box of water was then trimmed so that the edges were at least 8 Å away from the closest peptide atom. All waters within 1.67 Å of the peptide were then removed and the box size was adjusted to match the density of water (0.997 g/mL) at 298 K.[53,54] The system was then relaxed by performing 3000 conjugate gradient energy minimization steps. At least ten 10 ns simulations with different random seed numbers were performed for each peptide (12 simulations for K41+T42 and 10 for other peptides). Each 10 ns simulation generated 10,000 structures and only structures generated in the last 9 ns were used to analyze the structure and properties of the β-hairpin. The hydrophobic contact surface area (HCSA) was calculated using Voronoi polyhedra method.[55,56] The polyhedra surrounding each atom were uniquely defined by using the Delauney tessellation[57] and two carbon atoms sharing a common polyhedron face are defined as being in contact.[56] The hydrophobic clusters were defined by the largest side-chain to side-chain contact network, as previously described.[29] Clusters are defined as the set of all the molecules are in contact with at least one other molecule in the cluster.

A hydrogen bond is considered to be present if the distance between the donor hydrogen and the acceptor oxygen is 2.6 Å or less and the bond angle formed by the acceptor oxygen, hydrogen, and the donor atom is greater than 120°. An ion pair is defined using 3.5 Å as the distance cutoff between the charged nitrogen of the amino

Table I
Thermal Unfolding and Sequences of G-Hairpin Peptide Variants

Name	Sequence[a] 41 47 56	Net charge at pH 7[b]	Apparent T_m (°C)[c]
G41 (wt)	G-E-W-T-Y-D-D-A-T-K-T-F-T-V-T-E	−3	1.3[d]
K41 (wt*)	K-E-W-T-Y-D-D-A-T-K-T-F-T-V-T-E	−2	11.4[d]
K41+A47	K-E-W-T-Y-D-A-A-T-K-T-F-T-V-T-E	−1	18.5 (0.2)
K41+T42	K-T-W-T-Y-D-D-A-T-K-T-F-T-V-T-E	−1	26.5 (0.2)
K41+Q42+A47	K-Q-W-T-Y-D-A-A-T-K-T-F-T-V-T-E	0	33.0 (0.3)
K41+T42+A47	K-T-W-T-Y-D-A-A-T-K-T-F-T-V-T-E	0	35.5 (0.3)
			45.0 (0.3)(+20% methanol)

[a]The residue numbering corresponds to that for the intact protein G B1 domain.
[b]Calculated using standard pK values for the ionizable groups.[59]
[c]The apparent T_m values were determined by measuring chemical shifts of Tyr45-Hδ in 5 m*M* sodium phosphate in D_2O at pH 7. Values in parentheses show the standard errors in the fitting calculations.
[d]The apparent T_m values for G41(wt) and K41(wt*) were determined under identical conditions by Huyghues-Despointes *et al.*[29]

group and the oxygen of the carboxyl group. A salt-bridge interaction is considered to be present if it satisfies both the hydrogen bond and ion-pair definition.[29] The Ramachandran plot showing the turn main-chain ϕ, ψ angle distributions and the turn CαRMSD distributions are represented using the R package.[58]

RESULTS AND DISCUSSION

Peptide design

As described earlier, G-hairpin is a good model system to investigate many aspects of β-hairpin folding and stability. Here, we extend these studies to investigate the effects of long-range coulombic interactions on β-hairpin stability. G-hairpin has several electrostatic interactions that are predicted to be unfavorable at pH 7, so we constructed a set of four 16-residue G-hairpin variants (Table I) that have the unfavorable electrostatic interactions removed or altered. In summary, our design strategy had the following considerations: (1) All four variants include the replacement of Gly41 with Lys (G41K). This replacement was shown to introduce a salt bridge between the side chain of Lys41 and either the C-termini or side-chain carboxyl of Glu56, thus greatly enhancing the stability of the G-hairpin.[29] (2) Glu42 is replaced with either Gln or Thr, residues with polar but uncharged side chains and relatively high β-sheet propensities.[60,61] These substitutions were made to examine the effect of removing repulsive electrostatic interactions between Glu42 and Glu56 while still maintaining high overall β-sheet propensity. (3) A replacement of Asp47 with Ala at the first position of the β-turn, shown previously to stabilize the G-hairpin,[10] is used in three out of four variants. We seek to determine how this replacement stabilizes the β-hairpin because it not only removes the unfavorable interactions between the side-chain carboxyl groups of Asp47 and Asp46, but also removes favorable interactions between the carboxyl group of Asp47 and the amino group of Lys50.

Mutations can alter thermal stability

The folding rate of G-hairpin has been shown to be faster than the NMR time-scale ($>10^3$ s^{-1})[25,62]; therefore, the proton chemical shifts represent the populations of the folded and unfolded β-hairpin conformations at equilibrium.[29] The thermodynamics of G-hairpin[25] and several variants[10] have been determined by monitoring the temperature dependence of proton chemical shifts in 1D-NMR measurements. Importantly, Honda *et al.* have shown that the thermodynamic properties determined from the NMR probes on both the main-chain and the side-chains are similar and are identical to those determined from independent calorimetric experiments.[25] These results suggest that the thermal unfolding of G-hairpin can be adequately described by a cooperative two-state folding transition between folded β-hairpins and the unfolded state, consistent with results found for other G-hairpin variants.[26,27] These results provide enough evidences that the thermodynamic properties of our G-hairpin variants with same lengths can be determined by monitoring the temperature dependence of a single side-chain proton chemical shift.

Here we use the chemical shift changes of the Tyr45 Cδ protons with temperature as the probe to determine the relative thermal stabilities of the G-hairpin variants, as previously described.[10,29] 1D proton NMR spectra for all the G-hairpin variants (Fig. 1) were measured at pH 7 from 2 to 80°C. As controls, the melting curves for the wild-type G-hairpin and the K41 peptide (wt*) from a previous study are also shown.[29] All the melting curves show simple sigmoidal shapes, suggesting a two-state transition from folded to unfolded conformations with increasing temperature. The analysis of the thermal unfolding curves provides estimates for the melting tem-

 DOI 10.1002/prot

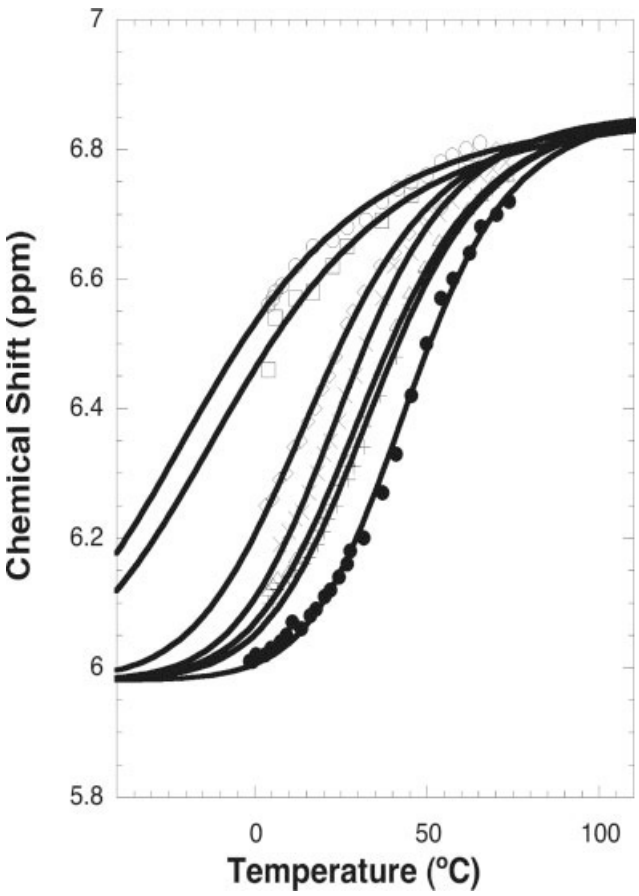

Figure 1

Thermal unfolding curves based on the chemical shifts change of the Tyr45-Hδ with temperature at pH 7 for each peptide: G41 (wt) (circles), K41 (wt) (squares), K41+A47 (diamonds), K41+T42 (crosses), K41+Q42+A47 (triangles), K41+T42+A47 (pluses), and K41+T42+A47 in 20% methanol (filled circles).*

peratures, apparent T_m (Table I). Peptides with higher apparent T_m values populate more β-hairpin structure and the stability of the peptides can be ranked according to their apparent T_m values: K41+T42+A47 ≈ K41+Q42+A47 > K41+T42 > K42+A47 > K41 (wt*) > wt. Single mutation D47A and G41K have been shown to stabilize the G-hairpin by ∼7°C[10] and ∼10°C[29] separately. For the double mutant K41+A47, an additive effect on β-hairpin stability was observed, providing an increase in apparent T_m from the wild-type G-hairpin of 17°C.[29] A single replacement of Glu42 with Gln shows an substantial increase in apparent T_m of ∼15°C as does the replacement of Glu42 with Thr, suggesting that a negatively charged residue is not favored at position 42.

Mutations can alter β-hairpin structure

The chemical shift dispersion in the 1D ^{1}H NMR spectra of these peptides is an excellent indicator of secondary structure formation. In particular, the deviations of the CαH chemical shifts from random coil values ($\Delta\delta_{C\alpha H}$) are useful parameters to characterize both α-helix and β-sheet structure.[20,63–66] Generally, upfield chemical shifts of CαH protons from random coil values (negative $\Delta\delta_{C\alpha H}$ values) are observed in helical and β-turn structures in proteins and peptides, whereas downfield shifts (positive $\Delta\delta_{C\alpha H}$ values) are observed in β-sheet conformations. The patterns we observe for $\Delta\delta_{C\alpha H}$ values for the peptides are consistent with two β-strands separated by a β-turn, as expected for the β-hairpin conformation.[64] In Figure 2, we compare the deviations of CαH chemical shift from random coil values for each residue in K41+Q42+A47, G-hairpin (G41),[1] K41 (wt*),[29] and the C-terminal region of the native intact PGB1 protein for comparison.[67] All the peptides have similar $\Delta\delta_{C\alpha H}$ values for each residue to those observed in the protein, but with a reduced magnitude. As expected, the patterns of $\Delta\delta_{C\alpha H}$ are in the same rank order in stability determined by the NMR thermal stability study (native β-hairpin in PGB1 > K41+Q42+A47 > K41 > G41). The $\Delta\delta_{C\alpha H}$ values for residues Asp46, Ala47, and Ala48 in the β-turn [Fig. 3(A)] show also an order that agrees with the stability rank (less negative values, less stable). The $\Delta\delta_{C\alpha H}$ values for residues Thr49 and Lys50, however, deviate substantially from those in the native protein [Fig. 3(A)]:[67] $\Delta\delta_{C\alpha H}$ for Thr49 is slightly positive in the protein but negative in all the peptides.

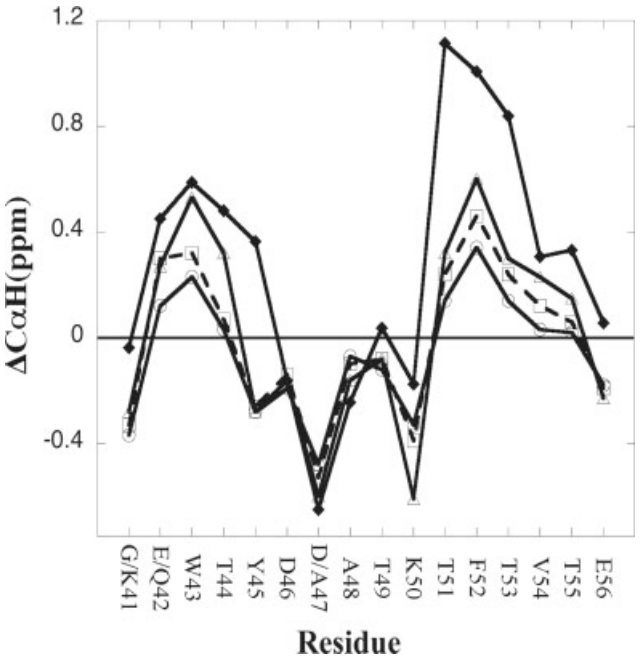

Figure 2

Deviations in CαH chemical shifts from random coil values for each residue in G41 (wt) (circles), K41 (wt) (squares), K41+Q42+A47 (triangles), and in the C-terminal region of PGB1 (filled diamonds)[29] in D_2O at pH 7 and 4°C.*

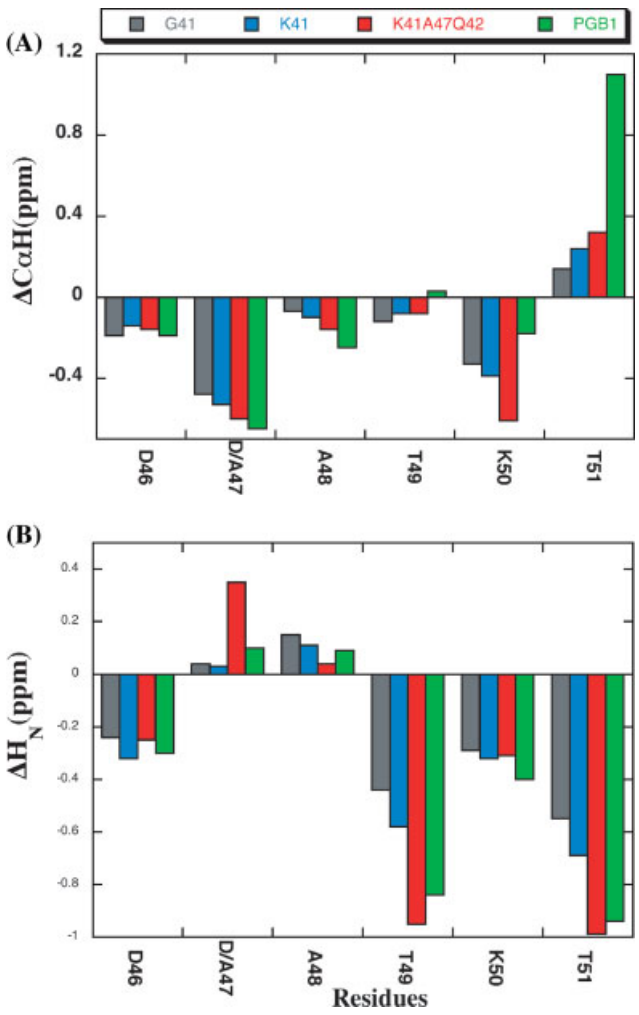

Figure 3

*Deviations in CαH (**A**) and H_N (**B**) random coil values for the turn residues in G41, K41, K41+Q42+A47, and the native PGB1. [Color figure can be viewed in the online issue, which is available at www.interscience.wiley.com.]*

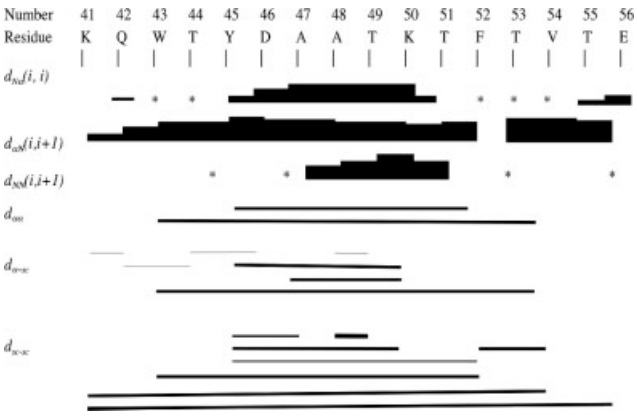

Figure 4

A summary of the NOE crosspeaks found in K41+Q42+A47 in 5 mM sodium phosphate 10% D_2O and 100% D_2O solutions at pH 7 and 4°C. The NOE intensities are proportional to the line thickness. Lines represent connectivities between two residues.

the D47A mutation has changed the conformations of the β-turn region of the G-hairpin variants.

A comparison of the short-range NOE contacts in K41+Q42+A47 with those in G41 and K41 confirms that the β-turn in the triple mutant has an altered conformation.[1,29] Figure 4 shows a summary of the relevant NOE data, and Figure 5 illustrates the NOE crosspeaks that are observed in K41+Q42+A47 but not in K41 or G41. According to the nomenclature of Thornton[69] and Richardson,[70] the β-hairpin in the protein adopts 4:4 hairpin conformation with a four-residue type IV turn, where the side-chain carboxyl group of Asp46 forms hydrogen bonds with the backbone NH groups of Thr51 and Lys50. In contrast, the NOE data for K41+Q42+A47 suggest the carboxyl of Asp46 forms hydrogen bonds with the backbone NH group of Thr49 and Lys50, consistent

This result suggests that the G-hairpin peptides adopt a different β-turn structure from that in the protein. Additionally, a larger change in $\Delta\delta_{C\alpha H}$ for Lys50 is observed in K41+Q42+A47 than in K41 or G41, and the $\Delta\delta_{C\alpha H}$ patterns of G41 and K41 in the β-turn region are quite different from $\Delta\delta_{C\alpha H}$ pattern of K41+Q42+A47 [shown in Fig. 3(A)]. To confirm the β-turn conformation change from 4:4 to 3:5 hairpin, we also examined the deviations of the backbone amide (H_N) chemical shifts from random coil values. As shown in Figure 3(B), the $\Delta\delta_{NH}$ of turn region in the triple mutant K41+Q42+A47 has a similar 3:5 hairpin chemical shifts deviation pattern to other 3:5 hairpins shown by Fesinmeyer *et al.*[68] Ala47 has a notable downfield shifted H_N comparing to that in K41 and in the native protein. In addition, the Thr49 and Thr51 have an enhanced upfield shifted H_N. All these results suggest that

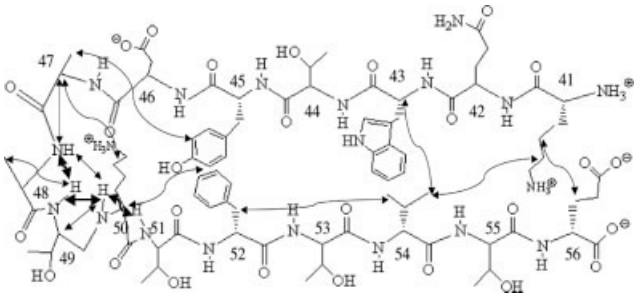

Figure 5

A summary of NOE interactions observed in the K41+Q42+A47 peptide but not in K41 or G41. The thickness of the arrows show the enhanced NOE interactions relative to those observed in K41 or G41.

DOI 10.1002/prot

with a 3:5 β-hairpin conformation. In addition, the pattern of $d_{NN}(i, i+1)$ NOE crosspeaks observed in K41+Q42+A47 are from Ala47 to Thr51 rather than from Asp46 to Thr51 as seen for K41 or G41, which suggests K41+Q42+A47 has a five-residue β-turn instead of a six-residue β-turn as in G41 peptide.[1] We observed intensity enhanced $d_{NN}(i, i+1)$ NOE interactions between Ala48 and Thr49, Thr49 and Lys50 and a more intense $d_{NN}(i, i+1)$ NOEs between Lys50 and Thr51. Moreover, a new $d_{NN}(i, i+2)$ NOE crosspeak is observed between Ala48 and Lys50, suggesting the turn is tighter in K41+Q42+A47. Taken together, these results suggest that the "AATKT" sequence in the triple mutant adopts a 3:5 β-hairpin, where the side chain of Lys50 rotates clockwise with respect to its position in the protein, extends in an upward direction perpendicular to the plane of the β-hairpin and packs against the side chain of Ala47. Consistent with this structure, we observe long-range NOE contacts between side-chain protons of Tyr45 and the CαH of Lys50 (Y45εH ↔ K50αH), CβH of Ala47 (Y45εH ↔ A47βH) and between the CαH of Ala47 and the side chain of Lys50 (A47αH ↔ K50γH) in the β-turn region (Fig. 5).

Three residue loops, like those in the 3:5 hairpin, are more prevalent in folded proteins than four residue loops,[2,20] which suggests the former may be more stable. This result is consistent with what we have observed here: replacement of Asp47 with the shorter side chain Ala47 leads to a 3:5 loop at the β-turn region and thus increases the stability of the β-hairpin. However, Asp has been shown to have much higher β-turn potential than Ala at the first turn position (i) in a statistical study of protein structures.[71] One obvious explanation for this discrepancy is that the statistical study was based on protein structures, not isolated peptides. In proteins, interactions of tertiary structures may stabilize certain β-turn conformations even energetically unfavorable ones, whereas in the absence of other interactions, β-turns can form more entropically favorable conformations. This may indicate that the contributions to β-turns in the proteins are not completely dependent on turn sequence, but could be context-dependent. We have observed here that the side chain of Lys50 orients differently from that in the protein due to the absence of interactions with other structural elements in the intact protein. Although the D47A replacement removes the favorable Asp47-Lys50 charge pair in the original sequence of G-hairpin, it also removes the steric clash between Lys50 and Asp47 in the β-turn. Thus, the D47A mutation leads to a new orientation for the side chain of Lys50, making a 3:5 β-hairpin and larger burial of hydrophobic surface in the G-hairpin.

K41+Q42+A47 retains the native-like G-hairpin register

It might be expected that the change of a "doubly bulged" turn (four residue 4:4 loop) to a three-residue (3:5) turn might lead to a one-residue frameshift in the alignment of β-strand register. However, the sharper bend of the β-turn toward the hydrophilic side in K41+Q42+A47 might compensate for this one-residue shift, thus maintaining the same register of the β-hairpin. In our case, this is supported by strong $d_{NN}(i, i+1)$ and weak $d_{\alpha N}(i, i+1)$ interactions in the β-turn residues and strong $d_{\alpha N}(i, i+1)$ in the β-strand residues (Fig. 4). Additionally, intense long-range interstrand αH ↔ αH NOE interactions between Trp43 and Val54 (Fig. 4), and between Tyr45 and Phe52 are still maintained, consistent with the proposed structure.

The β-hairpin variants have a more stable hydrophobic cluster

We observe more long-range NOE interactions of all types between main-chain and side-chain atoms as well as between different side chains in K41+Q42+A47 than in K41 or G41 (Fig. 5). In addition to the NOE contacts between the side chains of Phe52 and Trp43 observed in G41, we also observe strong NOE interactions between the side chains of Phe52 and Val54 (F52βH↔V54γH). In the K41+Q42+A47 peptide, new strong NOE contacts (Y45εH↔K50αH, A47αH↔K50γH) develop from the replacement of the hydrophilic residue Asp47 with a small hydrophobic residue Ala (Fig. 5 and see Supplement Materials). Furthermore, a NOE crosspeak is observed between the CαH of Trp43 and the side chain of Val54 (W43αH↔V54γH) and new NOE contacts between the side chains of Lys41 and Val54 (K41βH↔V54γH) and Glu56 (K41γH↔E56βH) are also observed (Fig. 5 and Supplement Materials). Together these results suggest K41+Q42+A47 has a more defined pleated β-hairpin structure with a larger hydrophobic cluster extending from the four-residue core (Tyr45, Trp43, Phe52, and Val54) to both the β-turn and the termini. The formation of this larger hydrophobic cluster formation is partly due to the new turn in 3:5 hairpin conformation, but also because of the more pleated hairpin structure in the variants. The more pronounced "pleated structure" not only helps to compensate for the one-residue shift of the new β-turn while maintaining a regular network of interstrand hydrogen bonding, it also helps to pack the hydrophobic side chains together better.

Removal of unfavorable electrostatic interactions stabilizes the β-hairpin

We observe long-range NOE interactions between Lys41 and the side chains of Val54 and Glu56 in the K41+Q42+A47 peptide. These contacts suggest that the ion-pair interactions at the termini are present as was observed previously for the K41 peptide.[29] The NOE contacts between the side chains of Lys41 and Val54 are only observed in K41+Q42+A47, but not in K41. Larger absolute $\Delta\delta_{C\alpha H}$ values for residue Val54, Thr55, Glu56 are also

Table II
Hydrophobic Contact Surface Area Between β-Hairpin Strands

Property	Category	G41	K41	K41+A47	K41+T42	K41+A47+T42	K41+A47+Q42
Strand HCSA[a] (Å^2)	Total[b]	91 ± 14	93 ± 18	93 ± 19	100 ± 15	104 ± 18	102 ± 13
	Cluster[c]	72 ± 15	75 ± 19	70 ± 19	78 ± 18	83 ± 20	81 ± 16

[a]The hydrophobic contact surface area (HCSA) between β-strands. Standard deviations are shown.
[b]The total is the average over a sum of all side-chain hydrophobic contacts.
[c]The cluster averages over only the largest cluster (see Materials and Methods).

observed in K41+Q42+A47 than those in K41 and the triple mutant is more stable than the single mutant. Therefore, the results suggest that removal of the charge-charge repulsion between Glu56 and Glu42 helps prevent the terminal residues from fraying, thus increasing the hydrophobic packing and stabilizing the β-hairpin.

Molecular dynamics study of the β-hairpin variants

In an effort to gain insight into the structural properties of the β-hairpins in solution and to visualize the nonnative 3:5 β-hairpin conformation, we have performed molecular dynamics simulations in explicit water for each peptide variant. All simulations were performed for 10 ns and several independent trajectories of β-hairpin behaviors for each peptide were generated.

A well-folded and stable β-hairpin should have a large amount of buried surface area from the interstrand interactions. To estimate the packing contributions from the mutations, we calculated the average total amount of buried HCSA and the HCSA in the major cluster of buried surface area. The side-chain packing in the peptides buries from 91 to 102 Å of HCSA (Table II) and the variants show increased side-chain packing with most of the increase in HCSA originating from the largest hydrophobic cluster (see Materials and Methods). The results show that the average amount of HCSA is largest in the triple mutants, consistent with the NOE data and suggest that the triple mutants (K41+T42+A47 and K41+Q42+A47) have more compact β-hairpin structures and thus more stability than the wild-type G-hairpin or the single or double mutants. Thus, we agree with previous studies that emphasized the important role of the hydrophobic cluster in the stability of the β-hairpin.[36,48,72–74]

Next, we used the NMR data as a guide to find the best representative structures from the MD simulations (Fig. 6). The best structures have the β-turn of a 3:5 hairpin with the hydrogen bonds between Asp46 carboxyl and Thr49 NH and Lys50 NH. The β-turn bends at residue Thr51 allowing for the hydrogen bond between Asp46 NH and Thr51 carboxyl and maintaining similar β-strand register as G-hairpin. In these structures, the β-hairpin has a compact hydrophobic cluster that extends from the central region to the β-turn and the termini, consistent with our experimental data.

Since some of the replacements we introduced are at the termini of the peptides, we also analyzed the generated ensembles to check the effects of varying the electrostatic interactions at the termini on the conformation of β-hairpins and compared the results to those on K41 and G41 from the previous study.[29] Table III shows the frequencies and types of the termini ion-pair interactions formed in our ensemble of structures. More than one type of ion-pair contacts (occupancy > 1.0) is observed in all the variants with the G41K replacement. The results show that

Table III
Terminal Ion Pair (IP) Interactions in the Ensembles of MD-Generated Structures

Property	Category	G41[a]	K41[a]	K41+A47	K41+T42	K41+Q42	K41+A47+T42	K41+A47+Q42
Terminal IP	Possible IP[b]	2	4	4	4	4	4	4
	IP[c]	0.6	1.1	1.3	1.3	1.8	1.2	1.2
	SB (%)[d]	92	78	100	100	100	97	100
Type of terminal IP[e]	Nm to Os	0.2	0.0	0.0	0.1	0.3	0.1	0.0
	Nm to Om	0.4	0.1	0.2	0.1	0.2	0.0	0.1
	Ns to Os	—	0.0	0.1	0.2	0.4	0.1	0.1
	Ns to Om	—	1.0	1.0	1.0	0.9	1.0	1.0

[a]The data for G41 and K41 are from Huyghues-Despointes *et al.*[29]
[b]The total number of potential ion pairs involving the N- and C-terminal residues.
[c]The average number of ion pairs in the ensemble structures.
[d]The percent occurrence that salt bridges form as well as ion pairs, defined by distance and angle restraints for hydrogen bonds.
[e]The type of potential terminal ion pairs include N-terminal (Nm) or Lys41 side chain amino group (Ns) to C-terminal (Om) or Glu56 side-chain carboxyl (Os). The dashes indicate not significantly populated.

DOI 10.1002/prot

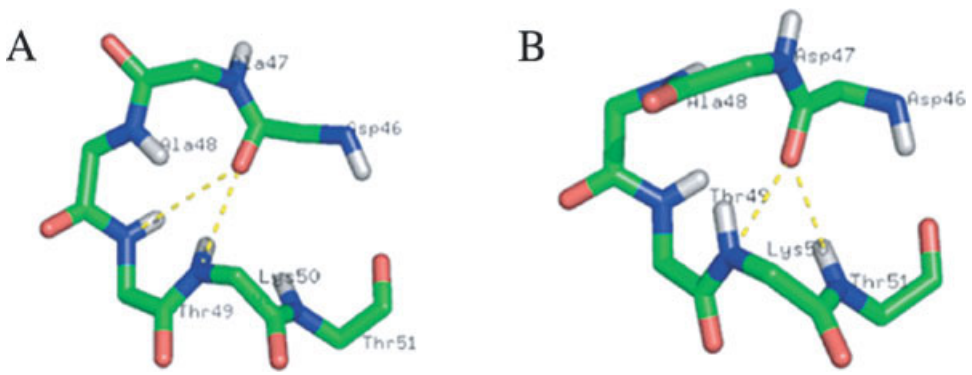

Figure 6

*Structural depictions of the native β-turn of 4:4 hairpin conformation of G-hairpin in PGB1 (**A**) and the β-turn of the nonnative 3:5 hairpin (**B**), generated from MD simulations. The hydrogen bonds between Asp46 carboxyl and Thr49 NH and Lys50 NH are shown.*

almost all the double and triple mutants form ion pairs all of the time (100% salt bridges). It is also found that removing the unfavorable charge–charge interaction between Glu42 and Glu56 seems to increase the occupancy of the ion pair between the side-chain amino group of Lys41 and the side-chain carboxyl of Glu56. From the selected MD-simulated structures for K41+Q42+A47 generated based on the NOEs data (Fig. 7), the β-hairpin tends to adopt a twisted and β-pleated structure to achieve the large hydrophobic cluster while keeping ion-pairs interactions at the termini.

To investigate the effect of replacement of Asp47 with Ala in the turn region, we calculated the CαRMSD values for all the ensembles of each variant. The crystal structure of G-hairpin in PGB1 was used as the starting structure for each MD trajectory and the reference for the CαRMSD calculation. The shape of the CαRMSD distribution represents how similar the structures are to the native structure of the G-hairpin in PGB1 and to each other. A single and narrow distribution peak indicates structures with less variation from the native G-hairpin, while a wide peak or more than one peak suggests differences from the native structure.[29] Figure 8 shows comparison of the distribution of turn region CαRMSD values of peptides with or without the D47A replacement. The results show that the variants with the D47A replacement have a broader and often

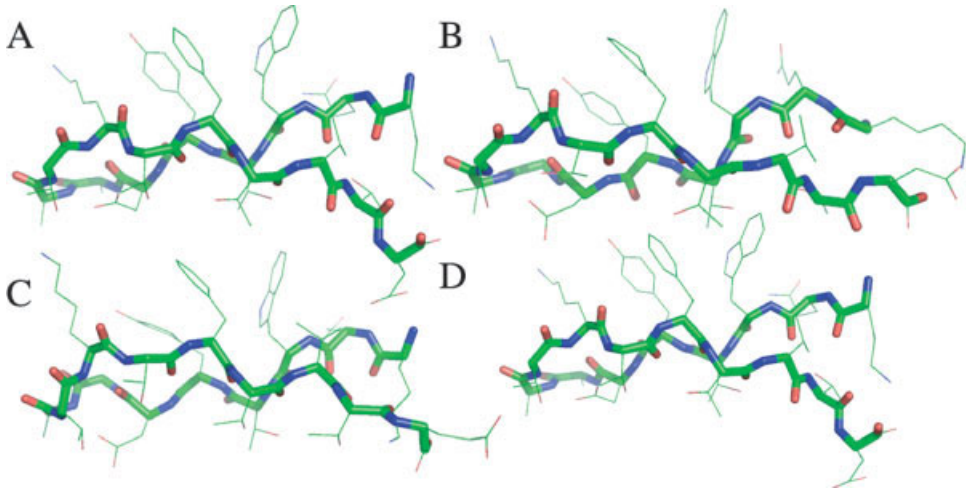

Figure 7

Representative of β-hairpin conformations of K41+A47+Q42 selected from MD-generated structures based on NOE data.

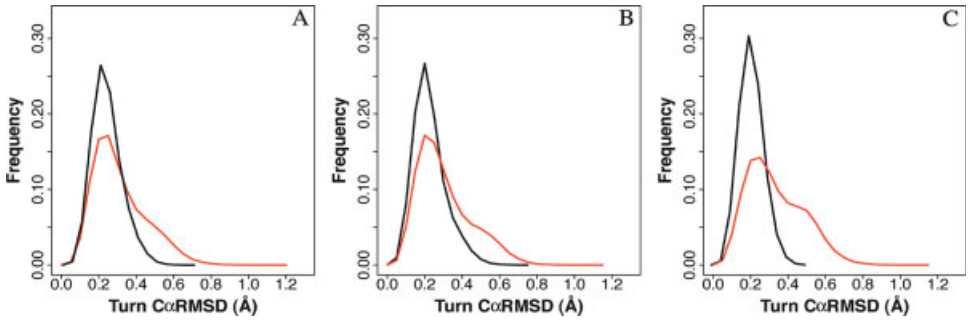

Figure 8

*Comparison of probability distributions of the normalized CαRMSD in the MD-generated ensembles in the β-turn region (residues 47–50) for: (**A**) K41 (solid line) and K41+A47 (dashed line); (**B**) K41+T42 (solid line) and K41+A47+T42 (dashed line); (**C**) K41+Q42 (solid line) and K41+A47+Q42 (dashed line). [Color figure can be viewed in the online issue, which is available at www.interscience.wiley.com.]*

show more than one peak in the distribution of turn region CαRMSD values, while the variants with the wild-type sequence in the turn region have a narrow and single peak. The larger CαRMSD values observed in the D47A variants suggest that this replacement changes the conformation of the β-turn in the hairpins, consistent with our experimental data.

Furthermore, according to the Ramachandran nomenclature for turns,[75] the central residues (i+1, i+2) in the loop of residues 47–51 (from position i to i+4) of a 3:5 type I turn will be expected to have an $\alpha_R\alpha_R$ conformation in Ramachandran plot, which is different from the miscellaneous type IV turn in the 4:4 hairpin. Also, the α_L conformation is quite common at position i+3 in type I turns.[71] Therefore, we also determined the distribution of the main-chain ϕ, ψ for the loop of K41+Q42+A47 hairpin based on the generated structures from MD simulations. In Figure 9, a loop conformation $\alpha_R\alpha_R\alpha_R\alpha_L\beta$ is populated for the sequence Ala47-Ala48-Thr49-Lys50-Thr51 in the K41+Q42+A47 variant as expected for type I turn. Previously, the Thornton group has also shown that type I β-turn is the most abundant turn type in folded proteins.[39,71] These results also suggest the type I turns are more favorable for β-hairpin formation.

CONCLUSIONS

Our data clearly show that removing the unfavorable charge-charge interactions can greatly increase the stability of β-hairpin. K41+T42+A47 is the most stable hairpin among all the studied variants and is ~96% folded in 20% methanol at 4°C. Consistent with a folded structure, we observe more NOE interactions between side chains near the termini and a more pleated β-hairpin structure with larger hydrophobic cluster in K41+Q42+A47 than in the other G-hairpin peptides. We also demonstrate the replacement of Asp47 with alanine in the turn region changes the β-hairpin conformation to a 3:5 hairpin without altering the register and also increases the thermal stability of the β-hairpin. This suggests that the β-hairpin conformation is strongly affected by the turn sequence and the cross-strand side-chain interactions. Importantly, our results show that removing unfavorable electrostatic interactions, even without introducing extra hydrophobic interactions, can enhance the cross-strand side-chain packing, and thus increase the stability of β-hairpin.

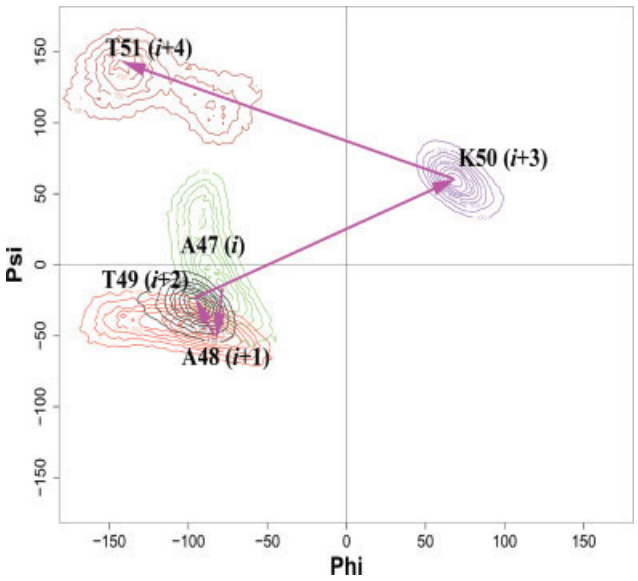

Figure 9

The Ramachandran plot showing the main-chain ϕ, ψ angle distributions for the five-residue loop (residues 47–51) in K41+Q42+A47 generated from MD simulations. The lines connect the most populated conformations (ϕ, ψ angles) for each residue in the turn. [Color figure can be viewed in the online issue, which is available at www.interscience.wiley.com.]

DOI 10.1002/prot

ACKNOWLEDGMENTS

We thank Dr. Xiaoming Kong from Biomolecular NMR Laboratory for helpful discussions regarding the NMR data, Xiaotao Qu for his help with programming and analyzing MD simulations, and Dr. Abbas Razvi for his helpful discussions. We also thank the Protein Chemistry Laboratory for assistance.

REFERENCES

1. Blanco FJ, Rivas G, Serrano L. A short linear peptide that folds into a native stable β-hairpin in aqueous solution. Nat Struct Biol 1994;1:584–590.
2. Searle MS, Williams DH, Packman LC. A short linear peptide derived from the N-terminal sequence of ubiquitin folds into a water-stable non-native β-hairpin. Nat Struct Biol 1995;2:999–1006.
3. Dill KA. Dominant forces in protein folding. Biochemistry 1990;29:7133–7155.
4. Kim PS, Baldwin RL. Intermediates in the folding reactions of small proteins. Annu Rev Biochem 1990;59:631–660.
5. Karplus M, Weaver DL. Protein folding dynamics: the diffusion-collision model and experimental data. Protein Sci 1994;3:650–668.
6. Bierzynski A, Kim PS, Baldwin RL. A salt bridge stabilizes the helix formed by isolated C-peptide of Rnase-A. Proc Natl Acad Sci USA 1982;79:2470–2474.
7. Shoemaker KR, Kim PS, Brems DN, Marqusee S, York EJ, Chaiken IM, Stewart JM, Baldwin RL. Nature of the charged-group effect on the stability of the C-peptide helix. Proc Natl Acad Sci USA 1985;82:2349–2353.
8. Bruch MD, Dhingra MM, Gierasch LM. Side chain-backbone hydrogen bonding contributes to helix stability in peptides derived from an α-helical region of carboxypeptidase A. Proteins 1991;10:130–139.
9. Ramirez-Alvarado M, Kortemme T, Blanco FJ, Serrano L. β-Hairpin and β-sheet formation in designed linear peptides. Bioorg Med Chem 1999;7:93–103.
10. Kobayashi N, Honda S, Yoshii H, Munekata E. Role of side-chains in the cooperative β-hairpin folding of the short C-terminal fragment derived from streptococcal protein G. Biochemistry 2000;39:6564–6571.
11. Ciani B, Jourdan M, Searle MS. Stabilization of β-hairpin peptides by salt bridges: role of preorganization in the energetic contribution of weak interactions. J Am Chem Soc 2003;125:9038–9047.
12. Espinosa JF, Munoz V, Gellman SH. Interplay between hydrophobic cluster and loop propensity in β-hairpin formation. J Mol Biol 2001;306:397–402.
13. Santiveri CM, Santoro J, Rico M, Jimenez MA. Factors involved in the stability of isolated β-sheets: turn sequence, β-sheet twisting, and hydrophobic surface burial. Protein Sci 2004;13:1134–1147.
14. Scholtz JM, Marqusee S, Baldwin RL, York EJ, Stewart JM, Santoro M, Bolen DW. Calorimetric determination of the enthalpy change for the β-helix to coil transition of an alanine peptide in water. Proc Natl Acad Sci USA 1991;88:2854–2858.
15. Chakrabartty A, Baldwin RL. Stability of β-helices. Adv Protein Chem 1995;46:141–176.
16. Williams S, Causgrove TP, Gilmanshin R, Fang KS, Callender RH, Woodruff WH, Dyer RB. Fast events in protein folding: helix melting and formation in a small peptide. Biochemistry 1996;35:691–697.
17. Hughes RM, Waters ML. Model systems for β-hairpins and β-sheets. Curr Opin Struct Biol 2006;16:514–524.
18. Griffiths-Jones SR, Maynard AJ, Searle MS. Dissecting the stability of a β-hairpin peptide that folds in water: NMR and molecular dynamics analysis of the β-turn and β-strand contributions to folding. J Mol Biol 1999;292:1051–1069.
19. de Alba E, Jimenez MA, Rico M. Turn residue sequence determines β-hairpin conformation in designed peptides. J Am Chem Soc 1997;119:175-183.
20. de Alba E, Rico M, Jimenez MA. Cross-strand side-chain interactions versus turn conformation in β-hairpins. Protein Sci 1997;6:2548-2560.
21. de Alba E, Jimenez MA, Rico M, Nieto JL. Conformational investigation of designed short linear peptides able to fold into β-hairpin structures in aqueous solution. Fold Des 1996;1:133–144.
22. Santiveri CM, Pantoja-Uceda D, Rico M, Jimenez MA. β-Hairpin formation in aqueous solution and in the presence of trifluoroethanol: a (1)H and (13)C nuclear magnetic resonance conformational study of designed peptides. Biopolymers 2005;79:150–162.
23. Cox JP, Evans PA, Packman LC, Williams DH, Woolfson DN. Dissecting the structure of a partially folded protein. Circular dichroism and nuclear magnetic resonance studies of peptides from ubiquitin. J Mol Biol 1993;234:483–492.
24. Kobayashi N, Endo S, Munekata E. Conformational study on the IgG binding domain of protein G. Pept Chem 1993;1992:278–280.
25. Honda S, Kobayashi N, Munekata E. Thermodynamics of a β-hairpin structure: evidence for cooperative formation of folding nucleus. J Mol Biol 2000;295:269–278.
26. Cochran AG, Skelton NJ, Starovasnik MA. Tryptophan zippers: stable, monomeric β-hairpins. Proc Natl Acad Sci USA 2001;98:5578–5583.
27. Fesinmeyer RM, Hudson FM, Andersen NH. Enhanced hairpin stability through loop design: the case of the protein G B1 domain hairpin. J Am Chem Soc 2004;126:7238–7243.
28. Andersen NH, Olsen KA, Fesinmeyer RM, Tan X, Hudson FM, Eidenschink LA, Farazi SR. Minimization and optimization of designed β-hairpin folds. J Am Chem Soc 2006;128:6101–6110.
29. Huyghues-Despointes BM, Qu X, Tsai J, Scholtz JM. Terminal ion pairs stabilize the second β-hairpin of the B1 domain of protein G. Proteins 2006;63:1005–1017.
30. Sheinerman FB, Brooks CL, III. A molecular dynamics simulation study of segment B1 of protein G. Proteins 1997;29:193–202.
31. Munoz V, Henry ER, Hofrichter J, Eaton WA. A statistical mechanical model for β-hairpin kinetics. Proc Natl Acad Sci USA 1998;95:5872–5879.
32. Pande VS, Rokhsar DS. Molecular dynamics simulations of unfolding and refolding of a β-hairpin fragment of protein G. Proc Natl Acad Sci USA 1999;96:9062–9067.
33. Ma B, Nussinov R. Molecular dynamics simulations of a β-hairpin fragment of protein G: balance between side-chain and backbone forces. J Mol Biol 2000;296:1091–1104.
34. Zagrovic B, Sorin EJ, Pande V. β-Hairpin folding simulations in atomistic detail using an implicit solvent model. J Mol Biol 2001;313:151–169.
35. Tsai J, Levitt M. Evidence of turn and salt bridge contributions to β-hairpin stability: MD simulations of C-terminal fragment from the B1 domain of protein G. Biophys Chem 2002;101/102:187–201.
36. Espinosa JF, Syud FA, Gellman SH. Analysis of the factors that stabilize a designed two-stranded antiparallel β-sheet. Protein Sci 2002;11:1492–1505.
37. Pastor MT, Lopez de la Paz M, Lacroix E, Serrano L, Perez-Paya E. Combinatorial approaches: a new tool to search for highly structured β-hairpin peptides. Proc Natl Acad Sci USA 2002;99:614–619.
38. Dinner AR, Lazaridis T, Karplus M. Understanding β-hairpin formation. Proc Natl Acad Sci USA 1999;96:9068–9073.
39. Wilmot CM, Thornton JM. Analysis and prediction of the different types of β-turn in proteins. J Mol Biol 1988;203:221–232.
40. Sibanda BL, Blundell TL, Thornton JM. Conformation of β-hairpins in protein structures. A systematic classification with applications to modelling by homology, electron density fitting and protein engineering. J Mol Biol 1989;206:759–777.
41. Haque TS, Gellman SH. Insights on β-hairpin stability in aqueous solution from peptides with enforced type I' and type II' β-turns. J Am Chem Soc 1997;119:2303–2304.

42. McCallister EL, Alm E, Baker D. Critical role of β-hairpin formation in protein G folding. Nat Struct Biol 2000;7:669–673.
43. Grimsley GR, Shaw KL, Fee LR, Alston RW, Huyghues-Despointes BMP, Thurlkill RL, Scholtz JM, Pace CN. Increasing protein stability by altering long-range coulombic interactions. Protein Sci 1999;8:1843–1849.
44. Perl D, Mueller U, Heinemann U, Schmid FX. Two exposed amino acid residues confer thermostability on a cold shock protein. Nat Struct Biol 2000;7:380–383.
45. de Alba E, Blanco FJ, Jimenez MA, Rico M, Nieto JL. Interactions responsible for the pH-dependence of the β-hairpin conformational population formed by a designed linear peptide. Eur J Biochem 1995;233:283–292.
46. Ramirez-Alvarado M, Blanco FJ, Serrano L. Elongation of the BH8 β-hairpin peptide: electrostatic interactions in β-hairpin formation and stability. Protein Sci 2001;10:1381–1392.
47. Olsen KA, Fesinmeyer RM, Stewart JM, Andersen NH. Hairpin folding rates reflect mutations within and remote from the turn region. Proc Natl Acad Sci USA 2005;102:15483–15487.
48. Searle MS, Griffiths-Jones SR, Skinner-Smith H. Energetics of weak interactions in a β-hairpin peptide: electrostatic and hydrophobic contributions to stability from lysine salt bridges. J Am Chem Soc 1999;121:11615–11620.
49. Delaglio F, Grzesiek S, Vuister GW, Zhu G, Pfeifer J, Bax A. NMRPipe: a multidimensional spectral processing system based on UNIX pipes. J Biomol NMR 1995;6:277–293.
50. Cavanagh J, Fairbrother W, Palmer A, Skelton N. Protein NMR spectroscopy: principles and practice. San Diego: Academic Press; 1996. pp 167–168.
51. Levitt M, Hirshberg M, Sharon R, Daggett V. Potential energy function and parameters for simulation of the molecular dynamics of proteins and nucleic acids in solution. Comp Phys Commun 1995; 91:215–231.
52. Levitt M, Hirshberg M. Calibration and testing of a water model for simulation of the molecular dynamics of proteins and nucleic acids in solution. Comp Phys Commun 1997;91:215–231.
53. Vedam R, Holton G. Specific volumes of water at high pressures, obtained from ultasonic-propagation measurements. J Acous Soc Am 1968;43:108-116.
54. Grindley T, Lind JE, Jr. PVT properties of water and mercury. J Chem Phys 1971;54:3983–3989.
55. Gerstein M, Tsai J, Levitt M. The volume of atoms on the protein surface: calculated from simulation, using Voronoi polyhedra. J Mol Biol 1995;249:955–966.
56. Tsai J, Gerstein M, Levitt M. Simulating the minimum core for hydrophobic collapse in globular proteins. Protein Sci 1997;6:2606–2616.
57. Delauney, B. Sur la sphère vide. Bull Acad Sci USSR(VII), Classe Sci Mat Nat 1934;783–800.
58. Becker RA, Chambers JM, Wilks AR. 1988. The new S language. London: Wadsworth and Brooks/Cole.
59. Thurlkill RL, Grimsley GR, Scholtz JM, Pace CN. pK values of the ionizable groups of proteins. Protein Sci 2006;15:1214–1218.
60. Smith CK, Withka JM, Regan L. A thermodynamic scale for the β-sheet forming tendencies of the amino acids. Biochemistry 1994;33: 5510–5517.
61. Griffiths-Jones SR, Sharman GJ, Maynard AJ, Searle MS. Modulation of intrinsic ϕ, ψ propensities of amino acids by neighbouring residues in the coil regions of protein structures: NMR analysis and dissection of a β-hairpin peptide. J Mol Biol 1998;284:1597–1609.
62. Munoz V, Thompson PA, Hofrichter J, Eaton WA. Folding dynamics and mechanism of β-hairpin formation. Nature 1997;390:196–199.
63. Wüthrich K. NMR of proteins and nucleic acids. New York: Wiley; 1986. p 17.
64. Wishart DS, Sykes BD, Richards FM. The chemical shift index: a fast and simple method for the assignment of protein secondary structure through NMR spectroscopy. Biochemistry 1992;31:1647–1651.
65. Wishart DS, Sykes BD. Chemical shifts as a tool for structure determination. Methods Enzymol 1994;239:363-392.
66. Case DA, Dyson HJ, Wright PE. Use of chemical shifts and coupling constants in nuclear magnetic resonance structural studies on peptides and proteins. Methods Enzymol 1994;239:392–416.
67. Blanco FJ, Serrano L. Folding of protein-G B1 domain studied by the conformational characterization of fragments comprising its secondary structure elements. Eur J Biochem 1995;230:634–649.
68. Fesinmeyer RM, Hudson FM, Olsen KA, White GW, Euser A, Andersen NH. Chemical shifts provide fold populations and register of β hairpins and β sheets. J Biomol NMR 2005;33:213–231.
69. Sibanda BL, Thornton JM. β-Hairpin families in globular proteins. Nature 1985;316:170–174.
70. Richardson JS. The anatomy and taxonomy of protein structure. Adv Protein Chem 1981;34:167–339.
71. Hutchinson EG, Thornton JM. A revised set of potentials for β-turn formation in proteins. Protein Sci 1994;3:2207–2216.
72. Kiehna SE, Waters ML. Sequence dependence of β-hairpin structure: comparison of a salt bridge and an aromatic interaction. Protein Sci 2003;12:2657–2667.
73. Pastor MT, Gimenez-Giner A, Perez-Paya E. The role of an aliphatic-aromatic interaction in the stabilization of a model β-hairpin peptide. Chembiochem 2005;6:1753–1756.
74. Seshasayee AS, Raghunathan K, Sivaraman K, Pennathur G. Role of hydrophobic interactions and salt-bridges in β-hairpin folding. J Mol Model 2005;12:197–204.
75. Wilmot CM, Thornton JM. β-Turns and their distortions: a proposed new nomenclature. Protein Eng 1990;3:479–493.

 DOI 10.1002/prot